

**Supplementary Information***Sample Information***Supplementary Table 1.** Brush molecular weights ( $M_g$ ), polydispersities (PDI) and grafting densities ( $\sigma$ ) of polymers grafted on silica particles.

PS-grafted-Silica						
Grafting density ( $\sigma$ )	$\sigma=0.01$ (chains/nm <sup>2</sup> )		$\sigma=0.05$ (chains/nm <sup>2</sup> )		$\sigma=0.1$ (chains/nm <sup>2</sup> )	
	$M_g$ (kg/mol)	PDI	$M_g$ (kg/mol)	PDI	$M_g$ (kg/mol)	PDI
	25	1.20	17	1.05	24	1.04
	51	1.20	34	1.05	45	1.06
	115	1.28	106	1.07	100	1.10
	158	1.50	160	1.21	154	1.25

**Supplementary Table 2.** Matrix molecular weights (M) and homopolymer polydispersities (PDI) used in the preparation of nanocomposites.

PS matrix homopolymers	
M (kg/mol)	PDI
17	1.04
42	1.08
142	1.06
272	1.08

*TEM Analysis of Particle Morphology:* Annealed samples were embedded in an epoxy resin and the resulting sample blocks were microtomed using a Leica UCT microtome to yield samples of approximately 100 nm thickness. Single slot grids (2 x 1 mm slot size), which were coated with a formvar membrane, were used for the analysis of structures through consecutive sections. The sections were microtomed both normal and parallel to the sample surface. The resulting particle morphology was examined using a JEM-100 CX transmission electron microscope (TEM). We have also conducted TEM tomography using a Tecnai F20 (200kV FEG) electron microscope at the New York Structural Biology Center. Microtomed samples were carbon coated to provide stability against the 200kV electron bombardment.

*USAXS Characterization of Particle Morphology:* Ultra-small angle x-ray scattering patterns were measured at the Advanced Photon Source at the 32ID-B beamline using a Bonse-Hart camera. Samples were approximately 2mm in diameter. Since the thicknesses varied from sample to sample (and sometimes within each sample, due to limitations in sample amounts), we do report scattering intensity in absolute units. The data were fit to the Beaucage unified

equation:<sup>1</sup> 
$$I(q) = \sum_i A_i \exp[-q^2 R_{gi}^2 / 3] + B_i \left[ \operatorname{erf} \left( \frac{q R_{gi}}{\sqrt{3}} \right) \right]^{p_i}$$
 where  $q$  is the wavevector, and

we assume several levels of structure (typically 2 or 3) to fit the data. When one assumes that the objects are spherical we can derive their radius from the relationship:  $R_g^2 = \frac{3}{5} R^2$ . The results obtained by fitting the data from the samples

shown in the first two rows of Fig. 2b are presented in Supplementary Table 3. The USAXS gives the size of the primary particles, and also indicates the existence of larger scale mass fractal structures (with fractal dimension  $\sim 3$ ). It is unclear why the particle sizes vary in the last three rows, while they remain relatively constant for the first three rows. We conjecture that this might represent local particle clustering. USAXS does not provide the dimensions of the large scale clusters seen in the second row of Fig. 2b (samples with brush molecular mass of 34 and 106 kg/mol. respectively). This indicates that the cluster sizes are larger than  $\approx 1 \mu\text{m}$ .

**Supplementary Table 3.** Primary particle and cluster sizes obtained from Beaucage unified fits to the USAXS data at different  $q$  regions for data shown in Fig. 2d.

<sup>2</sup> Brush $M_g$ (kg/mol)	High $q$ -Primary particle $R_g$ (Å)	Low $q$ -Cluster $R_g$ (Å)	Intermediate $q$ $R_g$ (Å)	Low $q$ -Power law exponent
25	45	869		3.6
51	53	847		4.0
158	56	6034	499	3.1
17	150	7150		3.6
34	139			3.5
106	227			3.6

*Eliminating other artifacts:* At this juncture it is important to rule out other obvious experimental artifacts. First, in previous work, we have determined that the level of sonication used to facilitate dispersion in solution causes very little changes in the molecular weights of the polymers. For a polystyrene of 92 kg/mol we found that sonication for 2 min reduced the molecular mass to 90 kg/mol.<sup>3</sup> We have also conducted dynamic light scattering of polymer grafted particle suspensions in benzene (0.256 mg/ml) after various sonication times (up to 6 min). We find that there is no measurable change in the hydrodynamic radii of the particles especially up to 2 min, which is the maximum time to which we subject our samples to sonication ( $R_h$  is 53 nm at 0min, 50 nm at 1 min and 54 nm at 2 min). We also rule out spatial anisotropies in the grafting of the polymer chains to the particles. Our previously published work,<sup>3,4</sup> which was obtained by casting a drop of tetrahydrofuran solution containing only the PS brush-grafted nanoparticles onto a TEM grid and then evaporating the solvent, shows no hint of any “string-like” or compact “dot-like” structures: rather, the particles appear to order into quasi-hexatic structures in spite of the relatively significant polydispersity in bare particle sizes ( $14 \pm 4$  nm). Electrophoretic mobility measurements show that the

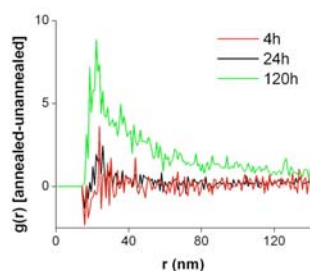
functionalized particles carry no measurable charge, and hence there are essentially no long-ranged charge effects.

We also tentatively rule out brush scission during the long annealings to which these nanocomposites are subject: in addition to the DLS experiments on the solution of particles (discussed above), we have redissolved the nanocomposites in solvent. GPC analysis of this solution gave no peak corresponding to the grafted chains that may have detached from the surface.

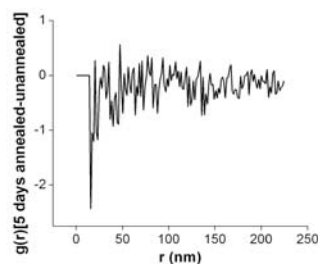
*Characterization of Domain Growth from TEM Studies:* The temporal change in dispersion is quantified by plotting  $\Delta g(r)$ , the difference in pair correlation function between the annealed sample and the unannealed composite (Supplementary Fig. 1 is derived from Fig. 2a: the miscible case is for the 42 kg/mol matrix, while the immiscible case is for the matrix with  $M=142$  kg/mol). These analyses are approximate in that we clearly have an anisotropic structure for the larger  $M$  matrix. Treating it as an isotropic structure, as is inherent in any analysis which only examines structures as a function of radial distance, loses any inherent anisotropy. With this caveat, in all cases, there is a slight negative feature close to contact: we conjecture that the particles are “squeezed” together in the casting process and move apart to allow the grafted chains to relax. Apart from this, the miscible case shows that  $\Delta g(r) \sim 0$  (Supplementary Fig. 1b) implying that particle dispersion does not change with annealing time. In contrast, the immiscible case shows a positive value of  $\Delta g(r)$  immediately after contact, with the height of the peak increasing with increasing annealing time. It is clear that the  $\Delta g(r)$  goes to zero at a characteristic distance, which is a measure of the size of particle agglomerates at that time. Supplementary Fig. 1c shows that the cube of this characteristic distance varies linearly with time, consistent with early time phase separation. (Note that the characteristic sizes presented here are corrected for the thickness of the TEM slice,  $\approx 100$  nm).

**Supplementary Figure 1.** Difference in pair correlation functions,  $\Delta g(r)$ , calculated from TEM images between **a.** 4h, 24h and 120h annealed and unannealed composites in 142 kg/mol PS matrix **b.** 120h annealed and unannealed composites in 42 kg/mol PS matrix. **c.** Cube of the distance between aggregating particles increases linearly with time in 142 kg/mol composite.

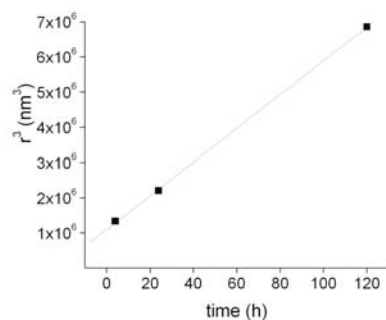
**a**



**b**



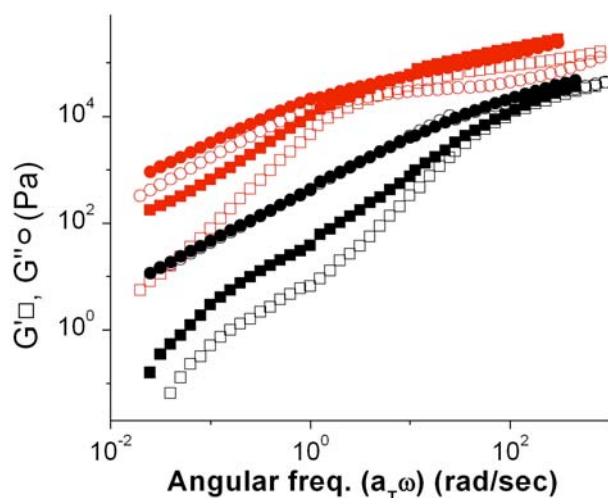
**c**



*Rheology:* Composites containing 5 mass% silica particles were prepared as discussed in the **Methods** section and then annealed for 5 days at 150°C under vacuum. Subsequently, they were kept in a vacuum oven at 70°C for two weeks to ensure that they were fully dried. After this, they were compression molded

with a vacuum assisted fixture at 150°C for an hour. Steady shear and dynamic oscillatory experiments were performed using a TA Instruments ARES rheometer under nitrogen with 8 mm parallel plates. The linear rheology data from three temperatures (130, 150 and 180°C) were superposed following the time-temperature superposition principle.

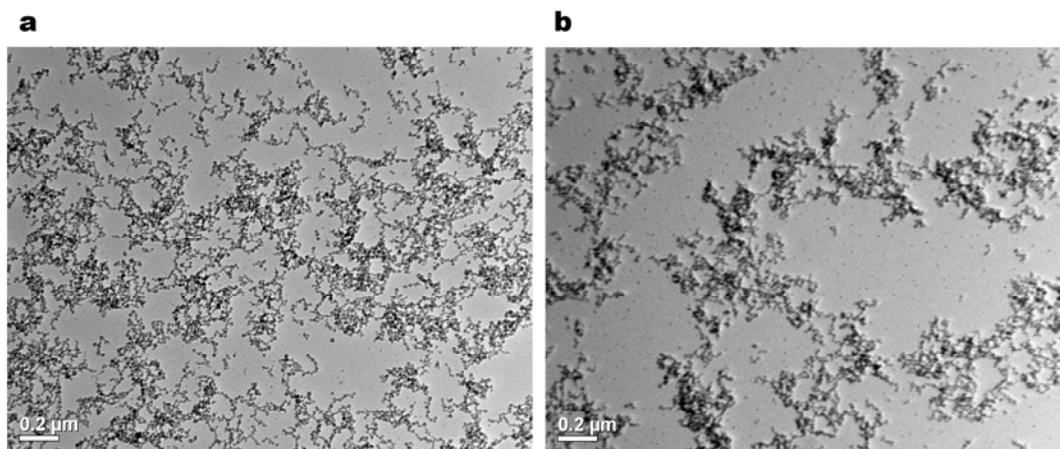
**Supplementary Figure 2.** Comparison of the storage ( $G'$ ) and loss ( $G''$ ) modulus of the PS composites containing 0 and 5 mass% silica particles in a matrix  $M=42$  kg/mol (black) and  $M=142$  kg/mol (red) as a function of the shifted frequency. Filled symbols refer to nanocomposites and open symbols are for matrix homopolymers. Master profile is obtained by time-temperature superposition at the reference temperature  $T=180^\circ\text{C}$ .



We select two samples corresponding to the images in Fig. 2a in the main text where the particles are grafted with 37 chains of  $M_g=106$  kg/mol: one with well dispersed short particle strings (matrix  $M=42$  kg/mol) and the other where there are large self-assembled particle sheets (matrix  $M=142$  kg/mol). The linear rheology of these nanocomposites (Supplementary Fig. 2) shows that the lower molecular weight matrix nanocomposite is analogous to a blend of linear and star polymers.<sup>5</sup> The relaxation at tens of rad/s is that of the linear homopolymer matrix and the relaxation at tenths of rad/s is that of (essentially) isolated spherical

nanobrushes, analogous to a slower relaxing star polymer. Thus, the storage modulus for example decreases strongly with decreasing frequency. The larger molecular weight matrix in stark contrast does not relax in the frequency range studied, instead exhibiting a much slower dependence on frequency. These results, which suggest that this latter sample behaves akin to a reversible gel, cannot be attributed to changes in polymer glass transition temperature due to the addition of particles: the  $T_g$  changes by less than 3K in all nanocomposites that we have measured.

**Supplementary Figure 3:** TEM micrographs of grafted nanoparticles with 37 chains/particle with  $M_g = 106$  kg/mol mixed with a homopolymer with  $M = 142$  kg/mol. The samples were only dried at  $70^\circ\text{C}$  after solution casting and not annealed at high temperatures. The left TEM is before the application of steady shear. The picture to the right has experienced a net strain of 270, which is well beyond the shear stress maximum.



*SANS for Characterization of Polymer Chains:* Samples of particles grafted with a hydrogenated brush of  $M_g = 130$  kg/mol with 37 chains per particle on average, were mixed with deuterated matrices. Both the amount of silica and the  $M$  of the matrix were varied in a series of experiments. As the neutron scattering length density of silica ( $2 \times 10^{10} \text{ cm}^{-2}$ ) is relatively close to the hydrogenated PS ( $1.5 \times 10^{10} \text{ cm}^{-2}$ ), SANS essentially measures the size of the particle with the brush chains

on them. Unfortunately due to the different contrasts in the system it is hard to unequivocally determine the size of the brush chains: the experiments reported here are thus only qualitatively indicative of brush dimensions. We have fit our SANS data, obtained at NCNR at NIST, Gaithersburg, MD, to the Beaucage model with two levels of structure as discussed above for the USAXS data analysis. The results indicate that  $R_g$  decreases when the matrix molecular weight is increased, while keeping the other parameters the same (e.g. grafting density at 0.26 chains/nm<sup>2</sup>, brush chain length at  $M_g = 130$  kg/mol and particle loading at 15 mass%) (Supplementary Table 4). These preliminary results support the idea of brush being “wet” when they are mixed with the lower molecular weight matrix, but “dewet” (followed by brush compression) for large  $M$  matrices. These findings are consistent with the recent work of Goel et al.<sup>6</sup>

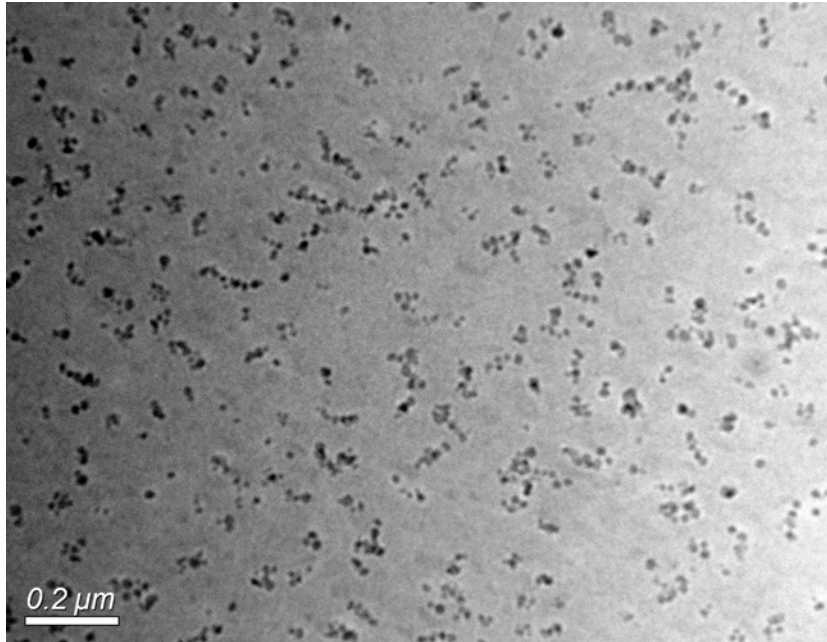
**Supplementary Table 4.** Nanobrush size within wetting and dewetting matrices measured using SANS.

$M_g$ brush (kg/mol)	$M$ matrix (kg/mol)	Mass % Silica	$R_g$ (particle+ brush) (Å)
130	90	15	169
130	200	15	119

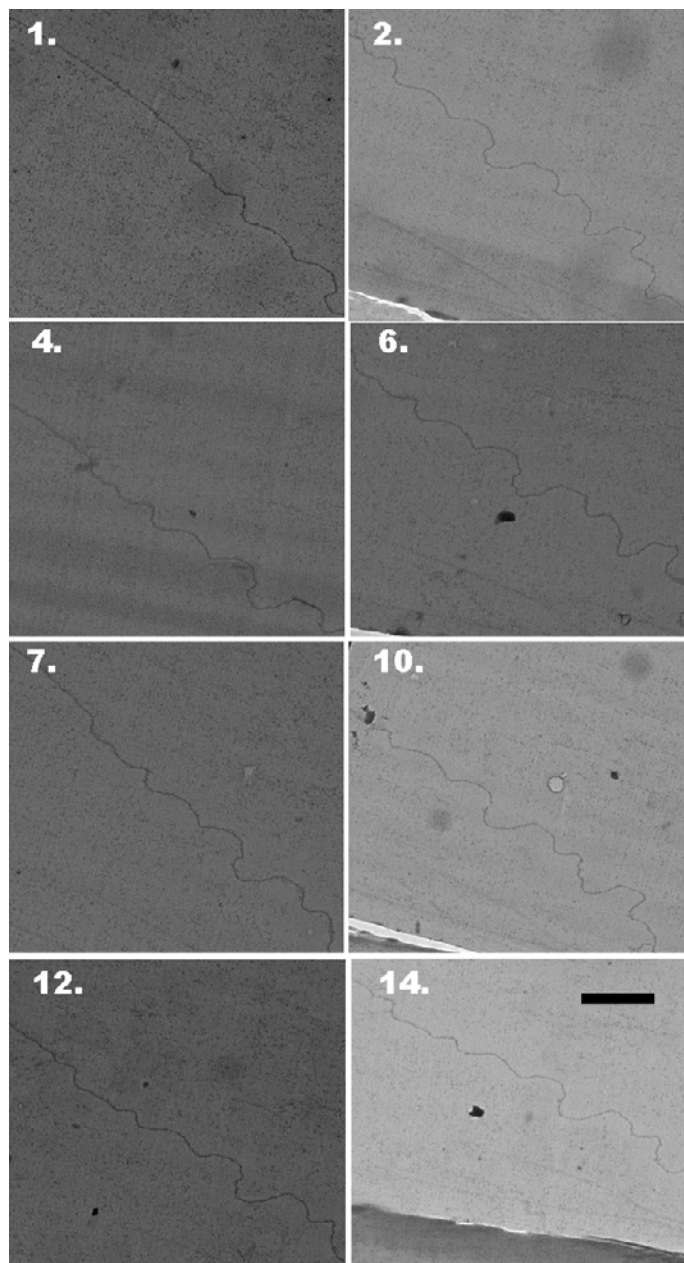
**Additional Figures:**

**Supplementary Figure 4. a.** Detailed TEM of 5 mass % silica grafted with a 106 kg/mol polystyrene brush, with polystyrene matrix of  $M = 17$  kg/mol annealed for 5 d. It is readily apparent that the particles form short strings. **b.** TEM micrographs of the blend of 5 mass % silica grafted with a 106 kg/mol PS in a 142 kg/mol PS homopolymer annealed for 5 d. from consecutive sections. Each section is approximately 100 nm thick. The numbers on the micrographs refer to the section number within a series of sections. The minimum lateral dimension of the sheet is determined by following the same structure in consecutive sections

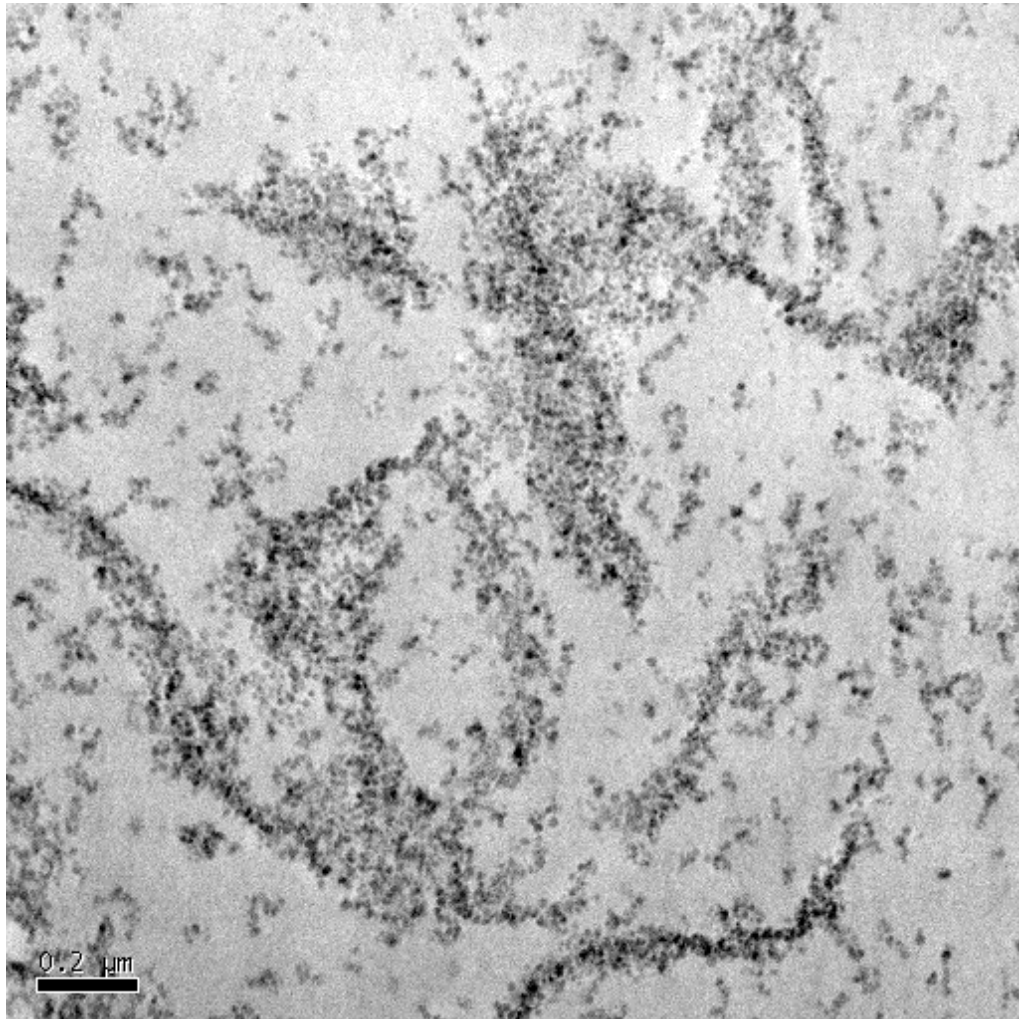
of the sample: we found that this sheet must be at least as large as  $1.4 \mu\text{m}$ . **c.** TEM micrograph of the composite with the  $142 \text{ kg/mol}$  matrix annealed for 5d. in Fig. 2a: In contrast to Fig. 2a, where the cutting direction was perpendicular to the sample surface, these samples were cut parallel to the surface plane of the sample. The scale bar is  $0.2 \mu\text{m}$ .

**a**

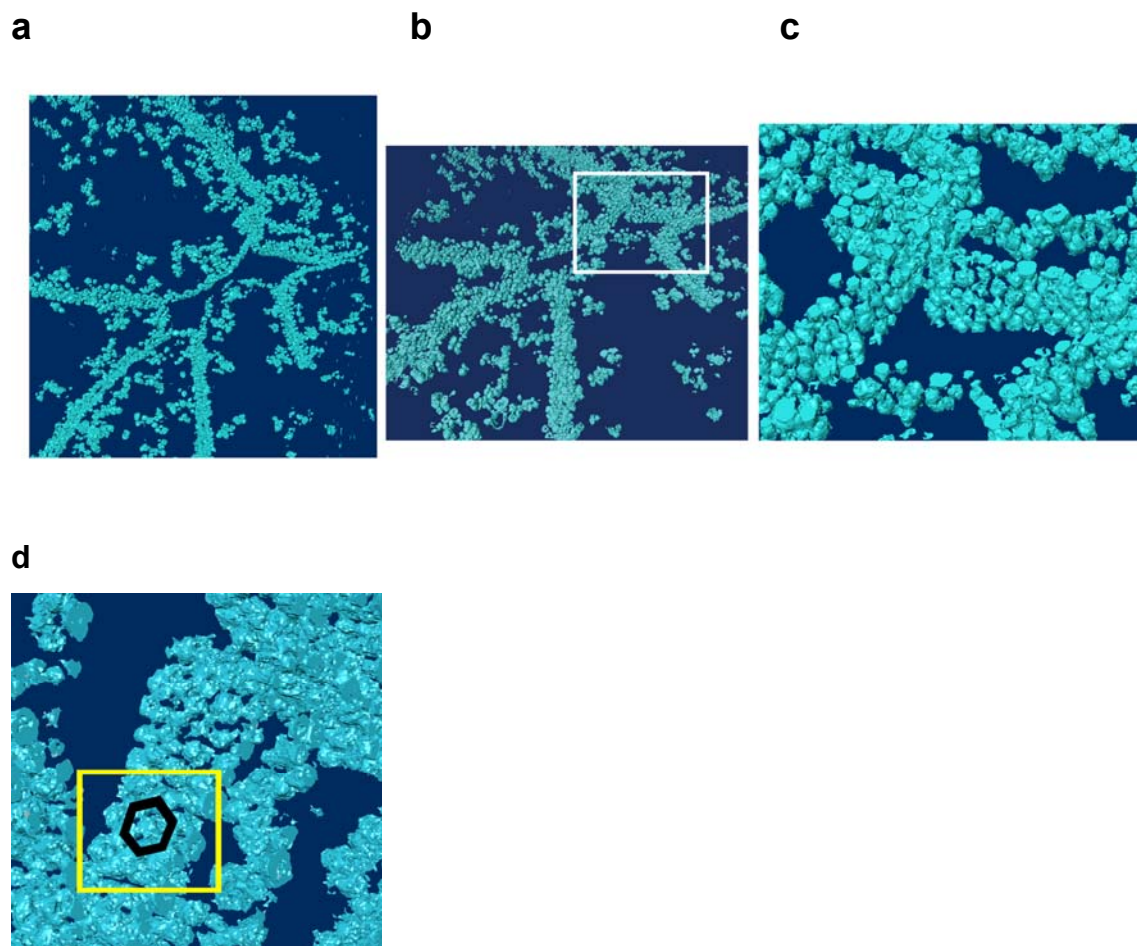
**b**



**c**



**Supplementary Figure 5. a.** 3-D organization of particles forming sheets within 142 kg/mol polystyrene matrix annealed for 5 d. The particles have 37 chains attached to them, on average, with  $M_g = 106$  kg/mol. Images represent one part of the series of slices along the 100 nm section. Particles form sheets with thickness of 2-3 particles. It is clearly seen that two sheets are stacked together in image **a**. **b.** The tilt view of the projection image. **c.** The magnified image of the selected region in **B**. **d.** Showing the hexagonal packing of particles.



**Supplementary Movie.** Movie of the same composite represents the sheet structures within a 100 nm thick section obtained from the construction of TEM tomograms.

## References

- 1 Beaucage, G., Approximations leading to a unified exponential power-law approach to small-angle scattering. *J Appl Crystallogr* **28**, 717 (1995).
- 2 Botti, A. et al., A microscopic look at the reinforcement of silica-filled rubbers. *J Chem Phys* **124** (17) (2006).
- 3 Bansal, A. et al., Quantitative equivalence between polymer nanocomposites and thin polymer films. *Nat Mater* **4** (9), 693 (2005).
- 4 Bansal, A. et al., Controlling the thermomechanical properties of polymer nanocomposites by tailoring the polymer-particle interface. *Journal of Polymer Science Part B-Polymer Physics* **44** (20), 2944 (2006).
- 5 Struglinski, M. J., Graessley, W. W., and Fetters, L. J., Effects of Polydispersity on the Linear Viscoelastic Properties of Entangled Polymers. 3. Experimental Observations of Linear and Star Polybutadienes. *Macromolecules* **21** (3), 783 (1988).
- 6 Goel, V. et al., Crystallization of Polymer Tethered Nanoparticles. *Preprint* (2008).